EIDGENÖSSISCHE TECHNISCHE HOCHSCHULE LAUSANNE
POLITECNICO FEDERALE LOSANNA
SWISS FEDERAL INSTITUTE OF TECHNOLOGY LAUSANNE

ÉCOLE POLYTECHNIQUE
FÉDÉRALE DE LAUSANNE

Faculty STI – Section of Microtechnology – Institute of Applied Optics
Mars 2002 to June 2002

Computation of custom made photonic crystals

Semester project

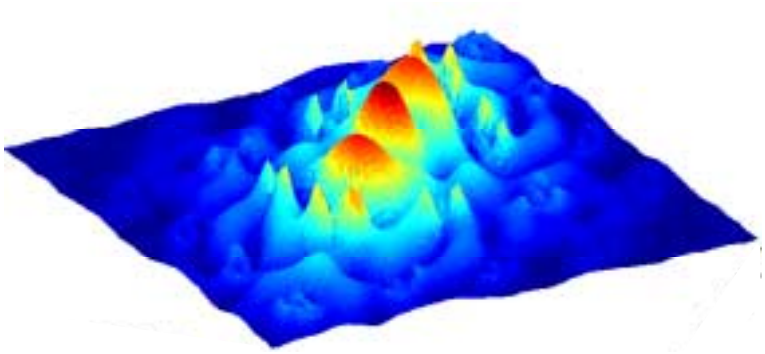

Marcel Leutenegger
Swiss Federal Institute of Technology Lausanne (EPFL), Switzerland, marcel.leutenegger@epfl.ch

Dr. Ivo Utke
Swiss Federal Institute of Technology Lausanne (EPFL), Switzerland, ivo.utke@epfl.ch

Prof. Olivier Martin
Swiss Federal Institute of Technology Zürich (ETHZ), Switzerland, olivier.martin@ifh.ee.ethz.ch

Prof. Patrik Hoffmann
Swiss Federal Institute of Technology Lausanne (EPFL), Switzerland, patrik.hoffmann@epfl.ch

EIDGENÖSSISCHE TECHNISCHE HOCHSCHULE LAUSANNE
POLITECNICO FEDERALE LOSANNA
SWISS FEDERAL INSTITUTE OF TECHNOLOGY LAUSANNE

ÉCOLE POLYTECHNIQUE
FÉDÉRALE DE LAUSANNE

Faculty STI – Section of Microtechnology – Institute of Applied Optics
Mars 2002 to June 2002

Abstract

The present paper concentrates on the theoretical understanding and the numerical computation of photonic crystals. It provides an introduction into the basic theory, shows some computation results and their interpretation by means of a few sample crystals, and proposes some measurement methods to evaluate the predicted behaviour. The interested user finds some additional software information, a couple of computation results and some images of an earlier made photonic crystal in the annexe.

In this work, the *MIT Photonic-Bands* software package was used for all of the numerical computations. The software was successfully installed on a personal workstation at home and on a server at the institute. Its capabilities and its functionality were tried out. The program was judged to work reliable. It yields the more accurate results the more time was spent for the computation, and it finds repeatedly the same results for the same task even on different machines and program versions. Then, the results were read in into *MatLab* for powerful post-treatment and graphical representation. For this reason, some self-programmed *MatLab* functions are also appended to the annexe.

A total of three photonic crystal samples were designed by numerical computation and layout. Each sample covers a particular function: a) a simple band gap filter, b) a high-Q cavity and c) an integrated wave-guide. It was shown that a high dielectric contrast is decisive to design large band gaps that are quite robust against fabrication errors.

Before spending more time for simulation, this work may be continued by fabrication and measure of the designed photonic crystals.

Lausanne, May 23, 2002

The author:

Marcel Leutenegger

Acknowledgements for assistance to:

Dr. Ivo Utke
Kay Hassler
Prof. Martin
Prof. Hoffmann
Prof. Lasser

Table of contents

Project brief

The technological advance in the miniaturisation of electronics asks for new materials always more performant and therefore pushes the research in this domain. By exploiting the formal analogy between electron and photon, researchers succeeded in designing and producing materials with astonishing optical properties: the so-called photonic crystals. Indeed, they could form the base of future zero threshold lasers, integrated optical fibres and low loss mirrors. This may allow overcoming the need for signal amplification at the end of optical fibres, great advance in telecommunications though possible application extend on the entire domain of optoelectronics.

By numerical simulation, this project aims to compute and model the optical properties of bidimensional photonic crystals grown on a plane, conductive surface by electron-induced deposition of a gas precursor. These crystals may be designed as frequency filters (band gap), wave-guides and so on. They can be deposited with the institute's scanning electron microscope. So, the customer can freely choose the crystal design provided he does not ask for feature sizes below 100nm.

Tasks:

Simulate the behaviour of some photonic crystals, model the effects and pass the results to Mr Adrian Bachmann for the fabrication of some test samples. Finally, it should be possible to verify the model by measuring the produced samples.

Theory: 70%
Praxis: 30%

Student:

Marcel Leutenegger
marcel.leutenegger@epfl.ch

Support:

Ass. Ivo Utke
ivo.utke@epfl.ch
021 693 51 81
BM–4.109

Prof. Olivier Martin
olivier.martin@ifh.ee.ethz.ch
01 632 57 22
ETZ–H6

Prof. Patrik Hoffmann
patrik.hoffmann@epfl.ch
021 693 60 18
BM–4.117

Delays:

Report
a hand out until 17^{00} on 21 June 2002 to Prof. Hoffmann, Prof. Martin and Mr Utke

Presentation
15´ presentation followed by 15´ discussion
begin at 14^{30} on 26 June 2002
room BM–5.202 at campus

1. Introduction

The perhaps first photonic crystals are commonly told Bragg reflectors. Although, the theoretical generalisation to multidimensional structures was done in the 1960's... the solutions could not be extracted analytically in a quite exact manner. Thus, it needed the appearance of powerful personal computers in the 1990's to make numerical calculation feasible at reasonable costs and computation time.

Nowadays, photonic crystals are easily designed through numerical simulation, but their realisation and test became the critical step. At some exceptions, the experimental work was made in the far infrared or even microwave range at wavelengths above 10µm. In contrast, the crystals made during this project are sensed to work in the visible range – in particular at the HeNe laser wavelength of 633nm. In consequence, the feature size is of the same scale, thus about 100nm to 500nm. Stepping down the wavelength to less than $1/10^{th}$ of the usual values expects nanotechnology for fabrication, high-resolution microscopy/interferometry during tests, and not at least other optical materials transparent for the visible light. On one hand, this complicates work, but on the other hand, at least the intensity distribution in the photonic crystals should be directly visible by microscopy.

What are photonic crystals?

Generally, people know about the solid-state physics, explaining for example the differences between electric isolators (ceramics, diamond...), semiconductors (Si, Ge, GaAs...) and conductors (metals). Most of the electrical phenomena deduce from the regular and periodic arrangement of atoms in conjunction with the atom's chemical properties. This defines the electronic band structure of the mentioned materials – all crystalline – and thus their electric properties.

Analogous, photonic crystals are made of several materials in a regular and periodic arrangement. Whereas the electrons in a crystal interact with the Coulomb potential of the atoms, the photons in a photonic crystal 'feel' the refractive indexes of the materials. This leads to a formally analogue description of the optical behaviour in terms of a photonic band structure. Note that the optical properties are controllable by the particular design of a photonic crystal, exactly like a semiconductor's electrical properties are controlled by the atom stochastic and their spatial arrangement.

Project goals

- Understanding the concepts, in particular the band structure and the associated analytical and numerical models.
- Numerical computation of 2D photonic crystals.
- Co-operation with Mr Adrian Bachmann for the fabrication of some particular samples and their measurement.
- Comparison of the measures and the computed predictions – if possible in a quantitative manner.

Framework

- Initiation of a new research domain at the institute.
- Implantation and test of some basic software tools.
- Provision of a "photonic crystals shorthand".

Applications

- Low loss mirrors as generalised Bragg reflectors extending the working range for either the incidence angle or the wavelength. This may be achieved through bi- or tridimensional photonic crystals.
- High Q laser cavities for zero threshold lasers.
- Wave-guides for integrated optics allowing very narrow curvatures.
- High Q wavelength filters. Could be used in telecommunications to split up a wavelength-multiplexed signal into its channels.
- Interaction of resonant structures with molecules. May be useful for the detection and identification of spurious chemicals or bio molecules present in a liquid.

2. Theory

The interaction of a radiation field with matter is the fundamental phenomena exploited in photonic crystals. It allows the designer of the crystal to control its optical properties in an exhaustive range. In fact, it took some time until researchers noted that the flow of photons is controllable in a manner similar to the flow of electrons in semiconductors.

Because of the strong analogy between semiconductors and photonic crystals, the reader is expected to have just an elementary knowledge of electromagnetism, quantum mechanics, solid-state physics and complex analysis. This chapter gives an introduction in the theory used for the present work. Far from being complete, the interested reader finds detailed information in the literature.

2.1 Basic problem

In a material with no free electric charges and no electric current, the Maxwell equations for electromagnetic fields lead to the following Helmholtz wave equations. Particularly, in free space:

$$\nabla\times\left(\nabla\times\vec{E}_{(\vec{r},t)}\right)=-\frac{1}{c^2}\frac{\partial^2}{\partial t^2}\vec{E}_{(\vec{r},t)} \qquad \text{where } c=\frac{1}{\sqrt{\varepsilon_0\mu_0}} \text{ is the velocity of light in free space} \tag{1}$$

$$\nabla\times\left(\nabla\times\vec{H}_{(\vec{r},t)}\right)=-\frac{1}{c^2}\frac{\partial^2}{\partial t^2}\vec{H}_{(\vec{r},t)} \tag{2}$$

If light travels in matter, its electric displacement is multiplied by the relative dielectric constant $\varepsilon_{(\vec{r})}$. At optical frequencies, magnetic materials are rare. So, this work exclusively treats dielectric materials with a relative magnetic constant assumed to be $\mu_{(\vec{r})}=1$. Hence, the Helmholtz equations transform to:

$$\frac{1}{\varepsilon_{(\vec{r})}}\nabla\times\left(\nabla\times\vec{E}_{(\vec{r},t)}\right)=-\frac{1}{c^2}\frac{\partial^2}{\partial t^2}\vec{E}_{(\vec{r},t)} \tag{3}$$

$$\nabla\times\left(\frac{1}{\varepsilon_{(\vec{r})}}\nabla\times\vec{H}_{(\vec{r},t)}\right)=-\frac{1}{c^2}\frac{\partial^2}{\partial t^2}\vec{H}_{(\vec{r},t)} \tag{4}$$

Seeking these equations by

$$\vec{E}_{(\vec{r},t)}=\vec{E}_{(\vec{r})}e^{-i\omega t} \qquad \text{and} \qquad \vec{H}_{(\vec{r},t)}=\vec{H}_{(\vec{r})}e^{-i\omega t} \tag{5}$$

leads to the angular frequency ω and the corresponding spatial fields $\vec{E}_{(\vec{r})}$ and $\vec{H}_{(\vec{r})}$ [1]. Then, the dispersion relation $d\omega=v_g\cdot dk$ (where v_g stands for the group respectively energy velocity) can be derived and the density of states approximated.

Note that the angular frequency is a global constant. This means that only elastic scattering is considered [2]. The angular frequency is in fact an eigenvalue of the wave equations and its corresponding fields are the related eigenfunctions. Hence, these eigenfunctions should satisfy the following eigenvalue equations:

$$\frac{1}{\varepsilon_{(\vec{r})}}\nabla\times\left(\nabla\times\vec{E}_{(\vec{r})}\right)=\frac{\omega^2}{c^2}\vec{E}_{(\vec{r})} \tag{6}$$

$$\nabla\times\left(\frac{1}{\varepsilon_{(\vec{r})}}\nabla\times\vec{H}_{(\vec{r})}\right)=\frac{\omega^2}{c^2}\vec{H}_{(\vec{r})} \tag{7}$$

Designing a photonic crystal is equivalent to layout a material with a periodic $\varepsilon_{(\vec{r})}$ such that the solutions of (3) and (4) follow the design specifications. In the case of simple functions like a sinusoidal $\varepsilon^{-1}_{(\vec{r})}$, it is possi-

1 The fields are noted as phasors – thus, an electric or magnetic field magnitude and a phase shift are assigned to each position.

2 In fact, inelastic scattering or fluorescence do affect the angular frequency but are not dealed with in this paper.

ble to perform an analytical study. For a general $\varepsilon_{(\vec{r})}$, only an iterative numerical design proofed feasible. Hence, for a given periodic $\varepsilon_{(\vec{r})}$, numerical calculation extracts solutions in a specified frequency range. In consequence, $\varepsilon_{(\vec{r})}$ is adapted and the calculation is relaunched until a suitable behaviour has been achieved.

2.2 Description of the crystal structure

Given a periodic material, it can be fully qualified by the definition of its base pattern and its periodicity. This description will show up very graceful, because it automatically minimises the number of parameters for numerical calculation.

Image 1 shows a bidimensional crystal. The crystal structure is represented by a set of base vectors and a corresponding pattern. The pattern is simply copied at each location reachable by an integer linear combination of the base vectors. For any integer *k* and *l*,

$$\vec{r}' = \vec{r} + \vec{T} \quad \text{with} \quad \vec{T} = k\vec{a} + l\vec{b} \quad (8)$$

points to a translation grid point where to copy the pattern to.

Note that the base vectors and the pattern are not unique. The pattern is called unit cell, whereas the translation grid is known as the crystal lattice. They are primitive, if for every point $\vec{r}$ and $\vec{r}'$, from where the crystal has the same structure, (8) is accomplished. The unit cell fills up the entire crystal volume by repetition on the lattice.

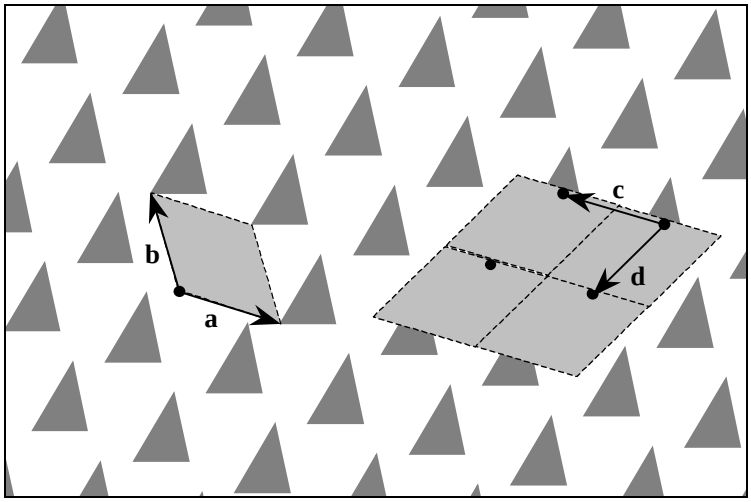

Image 1: Example of a 2D periodic structure.
The base pattern is bound on the translation grid spanned by the vector pairs $\vec{a}$ and $\vec{b}$, respectively $\vec{c}$ and $\vec{d}$. It is repeated at each grid point.

Note that the primitive lattice points and the primitive unit cell volume are invariant to any set of lattice vectors one chooses. Image 1 shows two of many possible choices: i) the vector pair ($\vec{a}$ / $\vec{b}$) and its unit cell attached on the grid points at its lower left corner, and ii) the vector pair ($\vec{c}$ / $\vec{d}$) with a unit cell attached somewhere in its inner region.

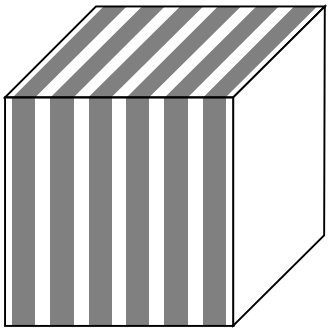

Image 2: Sample 1D crystal

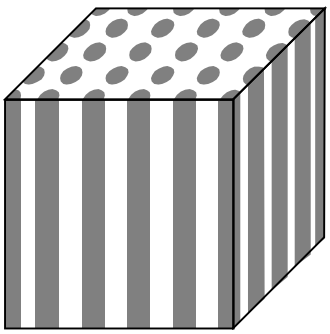

Image 3: Sample 2D crystal

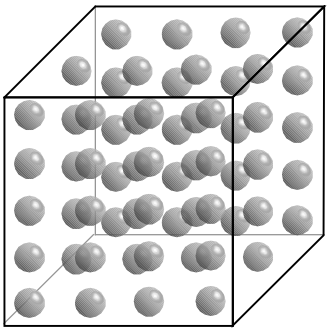

Image 4: Sample 3D crystal

2.3 Radiation modes ≡ eigenmodes of the photonic crystal

The eigenvalue equations (6) and (7) showed that any propagating electromagnetic wave is an eigenmode in the photonic crystal. Other modes cannot transverse long distances – indeed, they are evanescent modes [3].

[3] The material is considered to be free of absorption. Also, diffusion is not present – this means that only the variation of

As the crystal has a periodic function $\varepsilon_{(\vec{r})}$, the Bloch's theorem [4] can be applied to the eigenvalue equations. Therefore, $\vec{E}_{(\vec{r})}$ and $\vec{H}_{(\vec{r})}$ are characterised by a wave vector $\vec{k}$ in the first Brillouin zone and a band index *n*:

$$\vec{E}_{(\vec{r})} = \vec{E}_{\vec{k},n(\vec{r})} = u_{\vec{k},n(\vec{r})} e^{i\vec{k}\bullet\vec{r}} \qquad \text{where } u_{\vec{k},n(\vec{r}+\vec{T})} = u_{\vec{k},n(\vec{r})} \tag{9}$$

$$\vec{H}_{(\vec{r})} = \vec{H}_{\vec{k},n(\vec{r})} = v_{\vec{k},n(\vec{r})} e^{i\vec{k}\bullet\vec{r}} \qquad \text{where } v_{\vec{k},n(\vec{r}+\vec{T})} = v_{\vec{k},n(\vec{r})} \tag{10}$$

for any lattice translation $\vec{T}$

Because of the periodicity of the photonic crystal and the same periodicity of the solutions, it suffices to know the fields in one primitive unit cell. The global solution is then given by simple replication over the crystal lattice. Because of the fields' periodicity and continuity, they have to be equal on opposite boundaries of the unit cell.

Think of a wave travelling through the photonic crystal. Intuitively, it does not astonish that the wave's field reproduces the crystal period, such that it behaves in the same manner in each unit cell it encounters. In particular, this holds for non-absorbing crystals. But even if the wave is absorbed, it attempts to reproduce the crystal period while loosing intensity.

2.4 Expansion of the eigenvalue equations

Because $\varepsilon_{(\vec{r})}$ is periodic and any solution $\vec{E}_{(\vec{r},t)} = \vec{E}_{(\vec{r})} e^{-i\omega t}$ has the same spatial period, the eigenvalue equation (6) can be expressed in terms of Fourier series. First, generalise equation (8) to three dimensions:

$$\vec{T} = \sum_{i=1}^{3} l_i \vec{a}_i \qquad \text{where } \vec{a}_i \text{ are the lattice vectors and } l_i \in Z \tag{11}$$

In one dimension, the Fourier series would be expressed in terms of the base spatial frequency $b = \frac{2\pi}{a}$ and its harmonics $G = lb$. In three dimensions, this is rewritten as [5]:

$$\vec{G} = \sum_{i=1}^{3} l_i \vec{b}_i \qquad \text{where } \vec{b}_i \text{ are the reciprocal lattice vectors and } l_i \in Z \tag{12}$$

$$\text{such that } \vec{a}_i \bullet \vec{b}_j = 2\pi\delta_{ij} = \begin{cases} 2\pi & \text{if } i = j \\ 0 & \text{else} \end{cases} \tag{13}$$

The dielectric function $\varepsilon_{(\vec{r})}$ and equation (9) are now expanded in Fourier series:

$$\frac{1}{\varepsilon_{(\vec{r})}} = \sum_{\vec{G}} \kappa_{(\vec{G})} e^{i\vec{G}\bullet\vec{r}} \qquad \text{where } \kappa_{(\vec{G})} \text{ are the Fourier coefficients of } \varepsilon^{-1}_{(\vec{r})} \tag{14}$$

$$\vec{E}_{\vec{k},n(\vec{r})} = e^{i\vec{k}\bullet\vec{r}} \sum_{\vec{G}} \vec{E}_{\vec{k},n(\vec{G})} e^{i\vec{G}\bullet\vec{r}} \qquad \text{with the Fourier coefficients } \vec{E}_{\vec{k},n(\vec{G})} \tag{15}$$

Because the results are searched in terms of plane waves [see equation (9)], this method is called the planewave expansion method. Of course, solutions can be found by other base functions, such as spherical waves. Indeed, the spherical wave expansion method has proved its advantages for the numerical calculation

---

the relative electric constant scatters the wave.

4 The theorem holds for photonic crystals too. It originates from the description of the electron behaviour in the periodic electric potential due to the regular arrangement of atoms in crystalline solids. Bloch stated that the eigenfunctions of the Schrödinger equation for a periodic potential can be expressed as products of plane waves $e^{i\vec{k}\bullet\vec{r}}$ with corresponding functions $u_{\vec{k}(\vec{r})}$. These Bloch functions $u_{\vec{k}(\vec{r})}$ depend on the wave vector $\vec{k}$ and are periodic in the crystal lattice so that $u_{\vec{k}(\vec{r}+\vec{T})} = u_{\vec{k}(\vec{r})}$ for any lattice translation $\vec{T}$.

5 See "2.8 Real versus reciprocal lattice" on page 11.

of photonic crystals with cylindrical or spherical shapes in $\varepsilon_{(\vec{r})}$.

To complete the expansion, equation (6) is finally rewritten as:

$$\frac{1}{\varepsilon_{(\vec{r})}}\nabla\times\left(\nabla\times\vec{E}_{\vec{k},n(\vec{r})}\right)=\frac{\omega_{\vec{k},n}^2}{c^2}\vec{E}_{\vec{k},n(\vec{r})}$$

$$\left(\sum_{\vec{G}}\kappa_{(\vec{G})}e^{i\vec{G}\bullet\vec{r}}\right)\nabla\times\left(\nabla\times\sum_{\vec{G}'}\vec{E}_{\vec{k},n(\vec{G}')}e^{i\left(\vec{k}+\vec{G}'\right)\bullet\vec{r}}\right)=\frac{\omega_{\vec{k},n}^2}{c^2}\sum_{\vec{G}}\vec{E}_{\vec{k},n(\vec{G})}e^{i\left(\vec{k}+\vec{G}\right)\bullet\vec{r}}$$

$$\sum_{\vec{G}}\kappa_{(\vec{G})}e^{i\vec{G}\bullet\vec{r}}\sum_{\vec{G}'}\nabla\times\left(\nabla\times\vec{E}_{\vec{k},n(\vec{G}')}e^{i\left(\vec{k}+\vec{G}'\right)\bullet\vec{r}}\right)=\frac{\omega_{\vec{k},n}^2}{c^2}\sum_{\vec{G}}\vec{E}_{\vec{k},n(\vec{G})}e^{i\left(\vec{k}+\vec{G}\right)\bullet\vec{r}}$$

$$\sum_{\vec{G}}\kappa_{(\vec{G})}e^{i\vec{G}\bullet\vec{r}}\sum_{\vec{G}'}\nabla\times\left(i\left(\vec{k}+\vec{G}'\right)\times\vec{E}_{\vec{k},n(\vec{G}')}e^{i\left(\vec{k}+\vec{G}'\right)\bullet\vec{r}}\right)=\frac{\omega_{\vec{k},n}^2}{c^2}\sum_{\vec{G}}\vec{E}_{\vec{k},n(\vec{G})}e^{i\left(\vec{k}+\vec{G}\right)\bullet\vec{r}}$$

$$\sum_{\vec{G}}\kappa_{(\vec{G})}e^{i\vec{G}\bullet\vec{r}}\sum_{\vec{G}'}-\left(\vec{k}+\vec{G}'\right)\times\left(\left(\vec{k}+\vec{G}'\right)\times\vec{E}_{\vec{k},n(\vec{G}')}\right)e^{i\left(\vec{k}+\vec{G}'\right)\bullet\vec{r}}=\frac{\omega_{\vec{k},n}^2}{c^2}\sum_{\vec{G}}\vec{E}_{\vec{k},n(\vec{G})}e^{i\left(\vec{k}+\vec{G}\right)\bullet\vec{r}}$$

$$-\sum_{\vec{G}'}\kappa_{(\vec{G}-\vec{G}')}\left(\vec{k}+\vec{G}'\right)\times\left(\left(\vec{k}+\vec{G}'\right)\times\vec{E}_{\vec{k},n(\vec{G}')}\right)=\frac{\omega_{\vec{k},n}^2}{c^2}\vec{E}_{\vec{k},n(\vec{G})} \qquad (16)$$

The left hand side of equation (16) is computed up to a sufficiently large number *N* of $\vec{G}'$ and an eigenvalue problem is solved to extract the eigenvalue $\omega_{\vec{k},n}^2$. So, the dispersion relation $\omega_{n(\vec{k})}$ of the photonic crystal is obtained by computation of interesting frequency bands at some $\vec{k}$ points.

2.5 Proof of Bloch's theorem

First, the eigenvalue equation (6) in is rewritten as:

$$\nabla\times\left(\nabla\times\vec{E}_{(\vec{r})}\right)=\frac{\omega^2}{c^2}\varepsilon_{(\vec{r})}\vec{E}_{(\vec{r})} \qquad (17)$$

To pass to the Fourier domain, the dielectric function is expanded in a Fourier series and the electric field's eigenfunction as a Fourier integral:

$$\varepsilon_{(\vec{r})}=\sum_{\vec{G}}\varepsilon_{(\vec{G})}e^{i\vec{G}\bullet\vec{r}}$$

$$\vec{E}_{(\vec{r})}=\int\vec{A}_{(\vec{k})}e^{i\vec{k}\bullet\vec{r}}\,d\vec{k}$$

$$\nabla\times\left(\nabla\times\int\vec{A}_{(\vec{k})}e^{i\vec{k}\bullet\vec{r}}\,d\vec{k}\right)=\frac{\omega^2}{c^2}\sum_{\vec{G}}\varepsilon_{(\vec{G})}e^{i\vec{G}\bullet\vec{r}}\int\vec{A}_{(\vec{k})}e^{i\vec{k}\bullet\vec{r}}\,d\vec{k}$$

$$\int\nabla\times\left(\nabla\times\vec{A}_{(\vec{k})}e^{i\vec{k}\bullet\vec{r}}\right)d\vec{k}=\frac{\omega^2}{c^2}\sum_{\vec{G}}\int\varepsilon_{(\vec{G})}e^{i\vec{G}\bullet\vec{r}}\vec{A}_{(\vec{k})}e^{i\vec{k}\bullet\vec{r}}\,d\vec{k}$$

$$-\int\vec{k}\times\left(\vec{k}\times\vec{A}_{(\vec{k})}\right)e^{i\vec{k}\bullet\vec{r}}\,d\vec{k}=\frac{\omega^2}{c^2}\sum_{\vec{G}}\int\varepsilon_{(\vec{G})}\vec{A}_{(\vec{k}-\vec{G})}e^{i\vec{k}\bullet\vec{r}}\,d\vec{k}$$

$$\int\left(\vec{k}\times\left(\vec{k}\times\vec{A}_{(\vec{k})}\right)+\frac{\omega^2}{c^2}\sum_{\vec{G}}\varepsilon_{(\vec{G})}\vec{A}_{(\vec{k}-\vec{G})}\right)e^{i\vec{k}\bullet\vec{r}}\,d\vec{k}=0 \qquad (18)$$

This has to hold for all position vectors $\vec{r}$, so the integrand needs to vanish:

$$\vec{k}\times\left(\vec{k}\times\vec{A}_{(\vec{k})}\right)+\frac{\omega^2}{c^2}\sum_{\vec{G}}\varepsilon_{(\vec{G})}\vec{A}_{(\vec{k}-\vec{G})}=0 \tag{19}$$

Equation (19) implies, that all Fourier components $\vec{A}_{(\vec{k})}$ not related to the reciprocal lattice vectors are zero. This means that the electric field can be expressed in a Fourier series instead of a Fourier integral. Therefore:

$$\vec{E}_{\vec{k}(\vec{r})}=\sum_{\vec{G}}\vec{A}_{(\vec{k}-\vec{G})}e^{i\left(\vec{k}-\vec{G}\right)\bullet\vec{r}}=e^{i\vec{k}\bullet\vec{r}}\sum_{\vec{G}}\vec{A}_{(\vec{k}-\vec{G})}e^{-i\vec{G}\bullet\vec{r}}=\vec{u}_{\vec{k}(\vec{r})}e^{i\vec{k}\bullet\vec{r}} \tag{20}$$

The electric field is periodic with the same period as the dielectric function. In general, the number of Fourier components is not limited, so that equation (19) expands to an infinite set of eigenvalue equations. Hence, the eigenvalues and eigenfunctions are indexed by a subscript *n*.

Here, equation (9) has been showed. Of course, equation (10) can be proved in a similar manner.

2.6 Scaling laws

There are some useful properties of photonic crystals. Here, it will be shown that a uniform scaling of the spatial period, the time or the dielectric function results in a uniform scaling of the crystal's eigenfrequencies $\omega_{\vec{k},n}$.

First, given a uniform scale of the dielectric function:

$$\hat{\varepsilon}_{(\vec{r})}=m\varepsilon_{(\vec{r})} \qquad \text{where } m\in\Re>0 \tag{21}$$

Inserted into equation (17) leads to:

$$\nabla\times\left(\nabla\times\hat{\vec{E}}_{(\vec{r})}\right)=\frac{\hat{\omega}^2}{c^2}\hat{\varepsilon}_{(\vec{r})}\hat{\vec{E}}_{(\vec{r})} \tag{22}$$

By comparison with equation (17), the results can be derived immediately:

$$\underline{\underline{\hat{\omega}=\frac{\omega}{\sqrt{m}}}} \qquad \text{and} \qquad \underline{\underline{\hat{\vec{E}}_{(\vec{r})}=\vec{E}_{(\vec{r})}}} \tag{23}$$

Second, given a uniform scale of the spatial period and the time. If the scale factor *a* is the crystal's lattice size, the new variables $\hat{\vec{r}}$ and $\hat{t}$ are dimensionless:

$$\hat{\vec{r}}=\frac{\vec{r}}{a} \qquad \text{and} \qquad \hat{t}=\frac{c}{a}t \qquad \text{where } a\in\Re>0\ [\text{m}] \tag{24}$$

The Helmholtz equation (3) is transformed to:

$$\frac{1}{\varepsilon_{\left(\hat{\vec{r}}\right)}}\hat{\nabla}\times\left(\hat{\nabla}\times\hat{\vec{E}}_{\left(\hat{\vec{r}},\hat{t}\right)}\right)=-\frac{\partial^2}{\partial\hat{t}^2}\hat{\vec{E}}_{\left(\hat{\vec{r}},\hat{t}\right)} \qquad \text{where } \hat{\nabla} \text{ denotes the differentiation with respect to } \hat{\vec{r}} \tag{25}$$

This equation implies that its solutions can be linearly transposed to another crystal differing only in length but not in structure. Hence, a specific structure needs to be computed once and holds the solutions for any scaled structure. By convention, the computation is done for the normalised *k*-vectors $\hat{\vec{k}}$ and results in the normalised eigenfrequencies $\hat{\omega}$. They are then scaled to the considered crystal by:

$$\vec{k} = \frac{2\pi}{a}\hat{\vec{k}} \quad \text{and} \quad \omega = \frac{2\pi c}{a}\hat{\omega} \quad \text{where the factor } 2\pi \text{ has been inserted by convention [6]} \qquad (26)$$

2.7 Numerical computation

So far, the analytical computation of the dispersion relation in a photonic crystal has been showed. For numerical computation, the equations need to be discretizised. Equation (16) suggests an elegant solution. It relates the Fourier coefficients $\kappa_{(\vec{G})}$ of the inverse dielectric function $\varepsilon^{-1}_{(\vec{r})}$ **(14)** to the Fourier coefficients $\vec{E}_{\vec{k},n(\vec{G})}$ of the eigenfunction $\vec{E}_{\vec{k},n(\vec{r})}$ **(15)**. First, the volume of the crystal's unit cell is divided into *N* volume elements. For each element, $\varepsilon^{-1}_{(\vec{r})}$ is determined [7]. Then, the discrete Fourier transform yields the *N* coefficients $\kappa_{(\vec{G})}$. Thus, equation (16) expands into *N* linear equations at *N* coefficients each. A complete solution would mean to diagonalize a N^2 matrix – a time consuming task even for moderate *N* and just impossible for big *N*! Fortunately, in most cases, a partial solution – say *M* eigenvalues and eigenfunctions with $M << N$ – is sufficient for the analysis or the design of a photonic crystal. A subset of *M* eigenvalues can be computed much faster using a converging iterative eigensolver.

Note that the solution of equation (9) by use of equation (16) includes spurious zero modes that are not present for equation (10). Indeed, equation (10) maintains transversality [8], thus eliminating the zero modes. Advantageously, calculation is done for the magnetic field. Hence, the electric field can be derived by proportionality.

2.8 Real versus reciprocal lattice

To show the expansion of the eigenvalue equations, the reciprocal lattice was mentioned and its lattice vectors were given by equation (12). This section details the meaning of the reciprocal lattice and shows how it is linked to the crystal lattice.

Remind the commonly known Bragg grids. Indeed, they are 1D photonic crystals. The image 5 shows two examples with equal primitive lattices but different primitive unit cells.

Each unit cell reflects part of the incident light due to the modification of the dielectric constant. The total reflection is particularly high at all wavelengths that produce constructive interference between the reflected parts. On the other hand, the total transmission is particularly high at all wavelengths that give destructive interference between the reflected parts.

It may astonish that both Bragg grids reflect light mainly at the same wavelengths. Indeed, the unit cell pattern determines essentially the reflection efficiency for wavelengths around the 'exact' values where they themselves are determined principally by the lattice size *a* and the volumetric mean $\bar{\varepsilon}_{(\vec{r})}$.

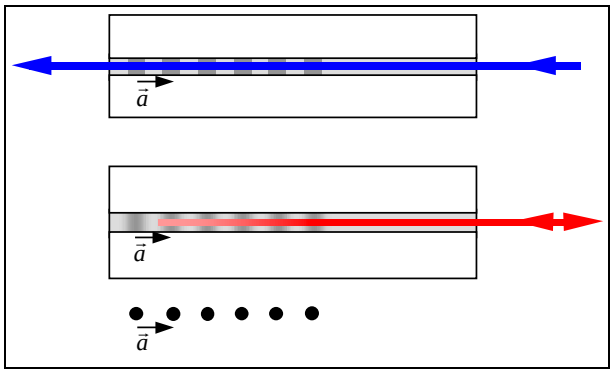

Image 5: Two Bragg grids in the core of an optical fibre. In this example, both have the same spatial period $\vec{a}$. Hence, both reflect the red light and transmit the blue one. The point grid below retains the spatial period but abstracts from the pattern.

---

6 $\hat{\vec{k}}$ and $\hat{\omega}$ are normalised to unity. The frequency is given by $f = \frac{c}{a}\hat{\omega}$ and the wavelength in the crystal by $\lambda = \frac{a}{\hat{k}}$.

7 This is a critical task! The solution's accuracy and the eigensolver's convergence speed are strongly modified by the manner of how the inverse dielectric function is attributed to the volume elements. See section 2.3 in "Block-iterative frequency-domain methods for Maxwell's equations in a planewave basis" for detailed info.

8 The magnetic field $\vec{H}_{\vec{k},n(\vec{G})}$ is always perpendicular to the vector $\vec{k}+\vec{G}$. See the proof at section 2.1 in "Optical Properties of Photonic Crystals".

Because of its dominant role, the lattice will be adjoined with its reciprocal representation in the *k*-space. In the case of the linear lattice $\vec{a}$, its reciprocal lattice is also linear with the lattice vector:

$$\vec{b} = \frac{2\pi}{a}\frac{\vec{a}}{a} = 2\pi\frac{\vec{a}}{\vec{a}\bullet\vec{a}} \qquad \text{so that } \vec{a}\bullet\vec{b} = 2\pi \tag{27}$$

The crystal lattice is a lattice in real space. Its lattice vectors are in units of length [m]. But the reciprocal lattice is a lattice in the *k*-space with inverse units [m^{-1}]. For example, imagine a plane wave propagating in the lattice direction:

$$\vec{E}_{(\vec{r},t)} = \vec{E}_0 e^{i\left(\vec{r}\bullet\vec{k}-\omega t\right)} \qquad \text{where } \vec{r}\|\vec{a} \text{ and } \vec{k}\|\vec{b} \tag{28}$$

$$\vec{E}_{(z,t)} = \vec{E}_0 e^{i\left(2\pi\frac{z}{\lambda}-\omega t\right)} \tag{29}$$

The scalar product $\vec{r}\bullet\vec{k}$ in the exponential is a product of a position vector $\vec{r}$ in the real lattice with a wave vector $\vec{k}$ in the reciprocal lattice. If the wave field is known only at the lattice points, a wave with wavelength λ_0 cannot be distinguished from any other with wavelength:

$$\lambda_n = \frac{an\lambda_0}{an+\lambda_0} \qquad \text{where } n \in Z \tag{30}$$

Inserted into equation (29), it can be seen that the exponential takes the same value on the lattice points at $z = ma$ with $m \in Z$. In fact, this is just a manifestation of Shannon's sampling theorem. In *k*-space, it can be written as:

$$\vec{k}_n = \vec{k}_0 + n\vec{b} \qquad \text{where } n \in Z \text{ and } \vec{k}_0 \in \left[-\frac{\vec{b}}{2},+\frac{\vec{b}}{2}\right] \tag{31}$$

The range of $\vec{k}_0$ is the so-called first Brillouin zone [9]. In the reciprocal lattice, the first Brillouin zone B_0 is nothing else than the unit cell that yields:

$$\int_{B_0}\vec{k}\bullet\vec{k}dB \xrightarrow{\text{change of } \partial B_0} \min \qquad \text{where } |B_0| \text{ is the constant volume} \tag{32}$$

and ∂B_0 the variable shape of the reciprocal unit cell

The concept of the reciprocal lattice can be applied to any 3D lattice as it was already mentioned in the equations (11) and (12). The scalar product of a lattice translation with a reciprocal lattice translation yields:

$$\vec{T}\bullet\vec{G} = \left(\sum_i l_i\vec{a}_i\right)\bullet\sum_j m_j\vec{b}_j = \sum_i\sum_j l_i\vec{a}_i\bullet m_j\vec{b}_j \tag{33}$$

Inserting equation (13) leads to:

$$\vec{T}\bullet\vec{G} = 2\pi\sum_i l_i m_i = 2\pi(\text{integer}) \qquad \text{because } l_i, m_i \in Z \tag{34}$$

This implies that plane waves with $\vec{k}$'s differing by $\vec{G}$ present the same fields on all lattice points $\vec{T}$. Indeed, equation (31) can be generalised to:

$$\vec{k} = \vec{k}_0 + \vec{G} \qquad \text{where } \vec{k}_0 \in B_0 \tag{35}$$

Note that the different waves have different energies. Hence, even if they seem to be identical on the lattice

---

9 Any wave with $\vec{k} \in \left(-\frac{\vec{b}}{2},+\frac{\vec{b}}{2}\right)$ sampled at the lattice points can be entirely reconstructed by interpolation.

points, their fields in the interior of the unit cell are well different. Indeed, the concept of the reciprocal lattice and the Brillouin zones will be very handy to represent the dispersion relation in a compact manner [10].

Given the lattice vectors, the reciprocal lattice vectors derive from equation (13). For example, the vector $\vec{b}_1$ stays perpendicular to the vectors $\vec{a}_2$ and $\vec{a}_3$. Hence it has to be parallel to $\vec{a}_2 \times \vec{a}_3$. Its projection on $\vec{a}_1$ has to be 2π, thus $\vec{a}_1 \bullet C(\vec{a}_2 \times \vec{a}_3) = 2\pi$. Solving for *C* yields:

$$\vec{b}_1 = 2\pi \frac{\vec{a}_2 \times \vec{a}_3}{\vec{a}_1 \bullet \vec{a}_2 \times \vec{a}_3} = 2\pi \frac{\vec{a}_2 \times \vec{a}_3}{V_0}$$
$$\vec{b}_2 = 2\pi \frac{\vec{a}_3 \times \vec{a}_1}{\vec{a}_2 \bullet \vec{a}_3 \times \vec{a}_1} = 2\pi \frac{\vec{a}_3 \times \vec{a}_1}{V_0} \qquad \text{where } V_0 \text{ is the volume of the unit cell} \qquad (36)$$
$$\vec{b}_3 = 2\pi \frac{\vec{a}_1 \times \vec{a}_2}{\vec{a}_3 \bullet \vec{a}_1 \times \vec{a}_2} = 2\pi \frac{\vec{a}_1 \times \vec{a}_2}{V_0}$$

Often, the constant 2π is omitted. So, be careful when interpreting the reciprocal lattice!

For 2D lattices, a third lattice vector $\vec{a}_3 \perp \vec{a}_1$ and $\vec{a}_2$ is introduced to apply the equations (36). The third reciprocal lattice vector $\vec{b}_3$ is then parallel to $\vec{a}_3$ although meaningless.

Image 6 shows a simple 2D rectangular lattice. Note that the first Brioullin zone B_0 is the surface around the lattice origin. It extends just to the first of the perpendicular bisectors that are drawn between the lattice origin and its neighbouring lattice points. This is the geometrical equivalent of condition (32).

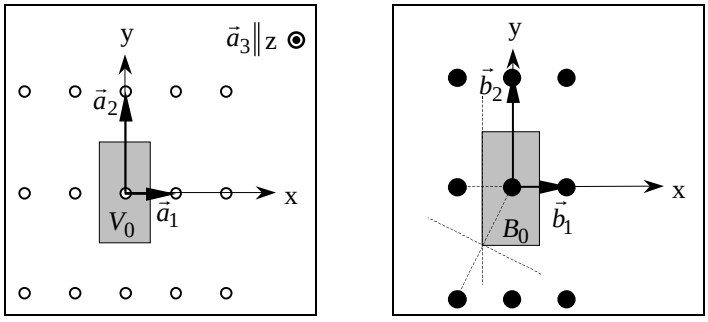

Image 6: Square lattice with lattice size *a* and its reciprocal lattice – also square with lattice size *b*. One of the unit cells and the first Brioullin zone are greyed.

2.9 Polarisation

In 1D photonic crystals, the crystal structure is strictly equivalent for both the electric and magnetic field. Hence, the solutions do not depend on polarisation.

In 2D photonic crystals, the dielectric constant varies in a plane. Now, the crystal structure differs for waves with different polarisation. Nevertheless, all solutions can be obtained from a superposition of two particular linear polarisations: a transverse electric (TE ≡ electric field in–plane) and a transverse magnetic (TM ≡ magnetic field in–plane) wave. Indeed, the electric field of the TM wave is always parallel to the structure variations. Hence, it has to be continuous across the material boundaries. On the other hand, the electric field of the TE wave is only partially parallel to the structure variations. Hence, its perpendicular part need not be continuous across boundaries.

In 3D photonic crystals, results depend on polarisation. Here, the polarisation is considered to be random, thus only yielding solutions for any polarisation.

2.10 Density of states

The density of states can be readily computed out of the total number of modes up to a specified quantum energy. In free space, the total number of modes up to an energy of $\hbar\omega_0$ in the volume V_0 is given by:

$$N_{(\omega_0)} = \frac{2V_0}{(2\pi)^3} \int_{k<\omega_0/c} d\vec{k} = \frac{2V_0}{(2\pi)^3} \frac{4}{3}\pi \left(\frac{\omega_0}{c}\right)^3 = \frac{V_0 \omega_0^3}{3\pi^2 c^3} \qquad (37)$$

where two orthogonal linear polarisations (independent) were considered.

[10] See "3.1 Band diagrams" on page 15.

The density of states is then:

$$D_{(\omega_0)} = \left.\frac{\partial N}{\partial \omega}\right|_{\omega=\omega_0} = \frac{V_0 \omega_0^2}{\pi^2 c^3} \qquad \text{in volume } V_0 \text{ (3D)} \tag{38}$$

$$= \frac{S_0 \omega_0}{\pi c^2} \qquad \text{on surface } S_0 \text{ (2D)} \tag{39}$$

$$= \frac{2L_0}{\pi c} \qquad \text{on distance } L_0 \text{ (1D)} \tag{40}$$

In the general case of photonic crystals, constant quantum energy does not describe a circular/spherical surface in the reciprocal space. Thus, the total number of modes and the density of states are more difficult to compute. Nevertheless, the density of states can be approximated if the speed of light *c* is replaced by the mean group velocity $\bar{v}_g$ for waves of the energy $\hbar\omega_0$.

3. Photonic band structures

This chapter deals with the representation of the dispersion relation by so called band diagrams. It should help to understand how to read out the characteristics of a photonic crystal – for example band gaps, group velocity or an approximation of the density of states.

3.1 Band diagrams

Remind the dispersion relation $d\omega = c \cdot dk$ in free space. It could be represented by a straight line in a ω-k-diagram like in graph 1. Now, introduce a periodic change of the dielectric constant in the x-direction. The modified dispersion relation $d\omega = v_g \cdot dk$ could be represented in the same diagram. This works fine for 1D problems. But, in the case of 2D or 3D crystals, how to represent the dispersion relation for different directions in the same graph?

Section 2.4 showed that the dispersion relation splits up in frequency sub-bands $\omega_{n(\vec{k})}$. And section 2.8 introduced the first Brioullin zone assigned to the reciprocal lattice.

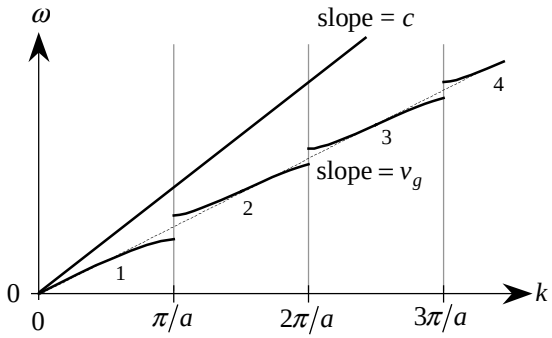

Graph 1: Dispersion relation in free space and for a 1D photonic crystal (Bragg reflector).

Hence, the spatial frequencies $k_2 = \pi/a + \Delta k$ in the second and $k_3 = 3\pi/a - \Delta k$ in the third Brioullin zone correspond to $k_1 = \pi/a - \Delta k$ in the first Brioullin zone! This is equivalent to fold graph 1 at the Brioullin zone boundaries. The result is the so-called band diagram showed in graph 2. By convention, for integer n, the spatial frequencies $k = n \cdot 2\pi/a$ are told the gamma point Γ and the X point stands for $k = (n + 0.5) \cdot 2\pi/a$. The dashed lines indicate the band structure of a homogeneous material, whereas the thick lines show the first four bands of a sample Bragg reflector.

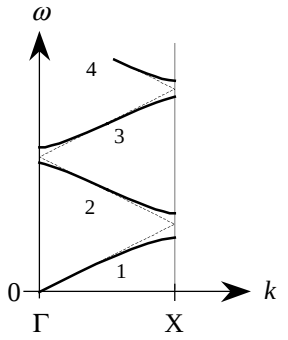

Graph 2: Band diagram

Caution:

Be careful when read out k-values, because the k-axis is not necessarily scaled uniformly! In this paper, the scaling is always the geometrical **path length** appearing in the reciprocal lattice.

3.2 Interpretation

Look at the examples in graph 2 and image 8. A band diagram directly shows a part of the dispersion relation of a photonic crystal. Image 8 shows the relation of $\omega_{(\vec{k})}$ on the boundary of the irreducible Brillouin zone. If a plane wave with frequency ω is incident on the crystal in one of the presented directions, the band diagram informs about its spatial wave vector $\vec{k}$. If the frequency ω falls in an ´empty´ range in its direction – a so called **partial band gap** – the crystal does not accept a propagating wave of that frequency and direction. Indeed, the crystal would add an imaginary contribution to ω, thus forcing the wave to be evanescent.

First, consider a propagating wave. The slope $d\omega/dk$ at the wave's $\left(\vec{k} / \omega_{(\vec{k})}\right)$ point gives the wave's **group and energy velocity** v_g in the crystal [11]. Whereas the group velocity is well defined, the phase velocity is not because of the difficulty to follow the propagation of a specified wave front (constant phase). As an example, look at the first band in image 8. For small $\vec{k}$ around Γ, the group velocity is nearly constant in all directions. But as $\vec{k}$ approaches M or X, the wave significantly slows down. Surprisingly, it stops propagating

[11] See section 2.5 in "Optical Properties of Photonic Crystals" for details on the relation of the phase, the group and the energy velocity in a photonic crystal.

at the M and X points [12]. Such "zero velocity" points are called **band edges**. The light they capture is said to be **frozen**.

Second, consider an evanescent wave. In the crystal, this wave cannot travel through long distances. Hence, it will be reflected rather than transmitted. The effect is very similar to the total internal reflection in dielectric wave-guides [13]. Frequency ranges where particular high reflection occurs are called band gaps. If the gap is present for any direction, it is a **full band gap** (like the light red zones in image 8), otherwise a **partial** one (light blue zone). Band gaps are always limited by band edges.

Besides, analysis shows that the wave penetrates the deeper into the crystal the more its frequency approaches a band edge.

How can we figure out the capacity of the crystal to transmit respectively reflect light? Look at graph 3. This is just another representation of the dispersion relation in image 8. The relationship of temporal and spatial frequency has been dropped in favour of a summary count of accepted modes – so called states.

The full band gaps are of course the zones with no states at all. On the other hand, the extremely flat bands at $f \approx 0.9$ show up in an increased state count. The state count is approximately proportional to the density of states and the crystals capacity of transmitting light, where the dispersion relation shows at which velocity transmission occurs.

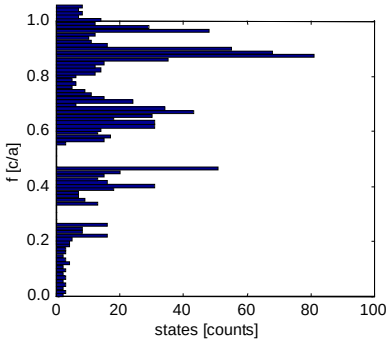

Graph 3: Modes of the example in image 8.

3.3 Square lattice

This lattice is highly symmetric because it is invariant to:

- rotations of integer multiples of 90° around the origin
- reflections at the x,y = 0,±0.5a and x = ±y axes
- point reflection at the origin

Because of symmetry, the first Brioullin zone can be reduced to an even smaller zone. If the dispersion relation has been computed for the irreducible Brioullin zone B_r, then it can be expanded by symmetry on the entire first Brioullin zone.

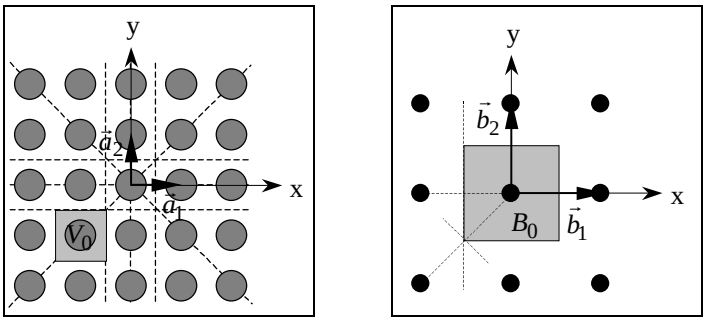

Image 7: Square lattice with lattice size *a* and its reciprocal lattice – also square with lattice size *b*. One of the unit cells and the first Brioullin zone are greyed.

[12] In praxis, quantum mechanics inhibits exact knowledge of ω and $\vec{k}$. Hence, the wave is always propagating even in a perfect crystal. If some absorption is present, it will advantageously weaken the bands definition (smear them out).

[13] Must not be confused! Total internal reflection occurs at the boundary from a 'denser' to a 'lighter' dielectric material. In contrast, the mean dielectric constant of a photonic crystal is generally higher than the one of the surrounding optical medium.

For example, the square lattice made of cylindrical rods keeps the lattice symmetry. Hence, the *k*-points X and Y are equivalent and need not to be computed separately.

Special points

The gamma point Γ: $\vec{k}_\Gamma = 0$ denotes always the origin of the reciprocal lattice.

$$\text{X}: \quad \vec{k}_\text{X} = \pm\frac{\vec{b}_1}{2}$$

$$\text{Y}: \quad \vec{k}_\text{Y} = \pm\frac{\vec{b}_2}{2}$$

$$\text{M}: \quad \vec{k}_\text{M} = \vec{k}_\text{X} \pm \vec{k}_\text{Y}$$

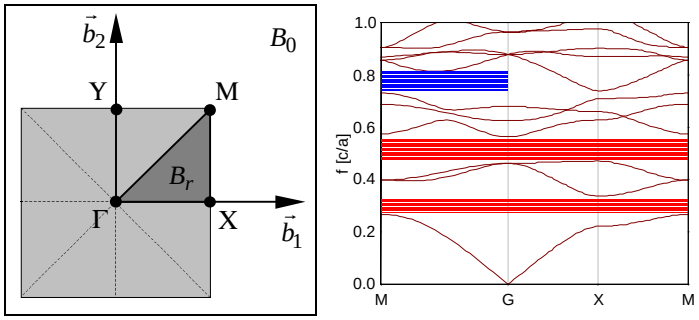

Image 8: a) First Brioullin zone with the irreducible Brioullin zone B_r darkened

b) TM band structure of a photonic crystal with a cylindrical rod of infinite height on every lattice point [14]. The rods have a radius $r = 0.3a$ and a dielectric constant $\varepsilon_r = 9$. They are set in air with $\varepsilon_r = 1$.

The first two complete band gaps are marked in light red, a partial band gap in light blue. Note the particularly flat bands at $f \approx 0.9$.

3.4 Triangular lattice

This lattice is also highly symmetric because it is invariant to:

- rotations of integer multiples of 60° around the origin
- reflections at the x,y = 0 axes and their replica rotated at ±30° around the origin
- point reflection at the origin

Because of symmetry, the first Brioullin zone can be reduced to a very small zone. If the dispersion relation has been computed for the irreducible Brioullin zone B_r, then it can be expanded by symmetry on the entire first Brioullin zone.

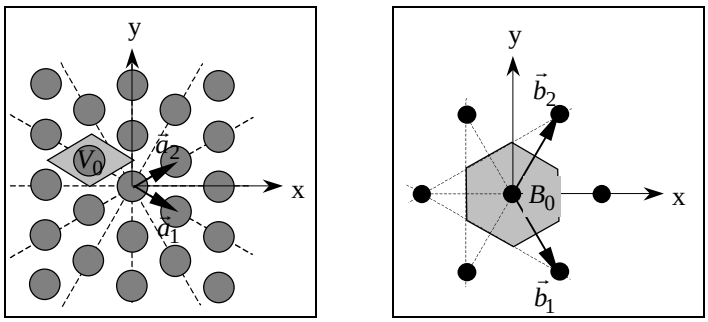

Image 9: Triangular (hexagonal) lattice with lattice size *a* and its reciprocal lattice – also triangular with lattice size *b*. One of the unit cells and the first Brioullin zone are greyed.

[14] See image 7.

For example, the triangular lattice made of cylindrical rods keeps the lattice symmetry.

Special points

The gamma point Γ: $\vec{k}_\Gamma = 0$ denotes always the origin of the reciprocal lattice.

$$M: \quad \vec{k}_M = \pm\frac{\vec{b}_1}{2}, \pm\frac{\vec{b}_2}{2}, \pm\frac{\vec{b}_1 + \vec{b}_2}{2}$$

$$K: \quad \vec{k}_K = \pm\frac{\vec{b}_1 - \vec{b}_2}{3}, \pm\frac{2\vec{b}_1 + \vec{b}_2}{3}, \pm\frac{\vec{b}_1 + 2\vec{b}_2}{3}$$

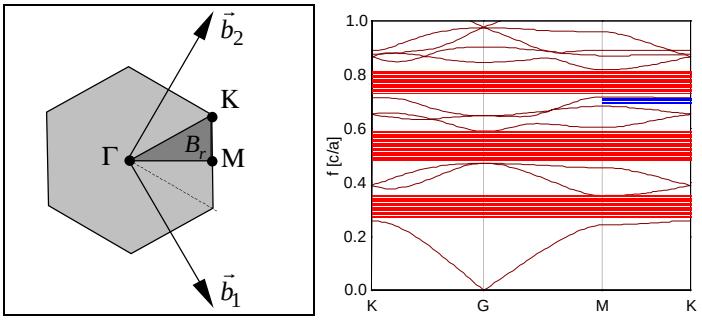

Image 10: a) First Brioullin zone with the irreducible Brioullin zone B_r darkened

b) TM band structure of a photonic crystal with a cylindrical rod of infinite height on every lattice point [15]. The rods have a radius $r = 0.3a$ and a dielectric constant $\varepsilon_r = 9$. They are set in air with $\varepsilon_r = 1$.

The first three complete band gaps are marked in light red, a partial band gap in light blue.

15 See image 9.

4. Examples of computed photonic crystals

This section presents some calculation results and their interpretation. Remind the goal behind these computations: predict the behaviour of some sample 2D photonic crystals designed for use at the HeNe laser wavelength. The sample structures had been restricted to square and triangular lattices – for computational ease [16] as well as to stay comparable with other works. A couple of graphs can be consulted in the annexe.

4.1 Square lattice with simple unit cell

The following results were computed for square lattices with size *a* and a single cylindrical rod in each unit cell. The rod is parallel to $\vec{a}_1 \times \vec{a}_2$, has a radius *r* and is made of a dielectric non-absorbing material with dielectric constant $\varepsilon = \varepsilon_r \varepsilon_0$. The unit cell is filled up with air.

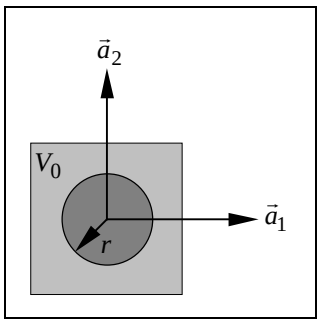

Image 11: Square lattice

Graph 4 shows the band gaps in function of the r/a ratio for a high ε-contrast of 11. Note the presence of several transverse magnetic (TM) band gap regions, whereas the transverse electric (TE) band gaps are nearly absent. In the 20th lowest bands, there is no full polarisation independent band gap.

The lowest TM band gap region is spanned by the 1st and 2nd tm bands. It has its largest relative range for $r \approx 0.2a$. Remind the method of computing the photonic bands: it has been showed that the ε_r^{-1} function is sampled and that the fast Fourier transform is taken. The extent of the lowest band gap depends mainly on the first Fourier coefficients representing the mean value and the main frequency. Indeed, for $r \approx 0.2a$, the main frequency coefficient is near its maximum to give rise to the first band gap's largest extent. The mean value determines mainly the mean band gap frequency. Hence, for increasing r/a, $\overline{\varepsilon_r^{-1}}$ decreases and the band frequencies do follow this decrease. Just remind that on a global view, the mean value $\overline{\varepsilon_r} = \overline{n}^{-2}$ is given by the mean refractive index *n*.

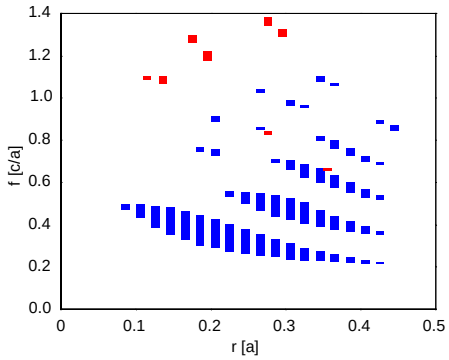

Graph 4: Gap map for $\varepsilon_r = 11$. TE band gaps in red and TM band gaps in blue.

Take a look at graph 5 now. A 1D photonic crystal has always full TE/TM band gaps for every thickness ratio between air and high ε regions! Well, the TE and TM modes cannot be distinguished in one dimension – they are both parallel to any modification of the dielectric constant. But, in contrast to the 2D crystal, the 1D crystal has a lot of large band gaps covering in total more frequencies than the propagating modes!

Why is the performance of the 2D crystal so 'bad'? Indeed, a wave travelling in the 1D crystal feels a unidirectional retroaction – coming from the partial reflections at the layer boundaries. In contrast, a wave propagating in the 2D crystal feels a bundle of weak reflections in all directions – scattered at the boundaries of the cylindrical rods. So, the retroaction takes place for an entire range of periods *a* to $\sqrt{2}a$ (*x*/*y* axis to the diagonal). This smooth retroaction narrows the full band gaps because a wave can 'choose' among different propagation directions to find a propagating mode. Hence, full 2D band gaps are only formed at high ε-contrasts enforcing the partial reflections!

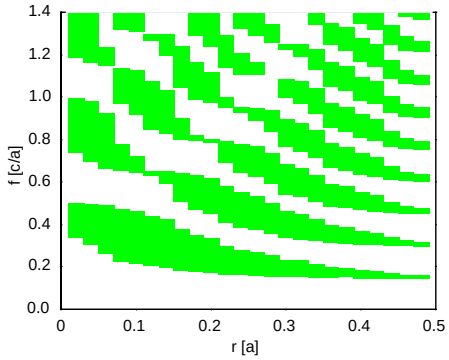

Graph 5: Gap map for $\varepsilon_r = 11$ and a 1D photonic crystal (linear lattice). TE/TM band gaps in green.

16 Because of the small and simple unit cell.

4.2 Triangular lattice with simple unit cell

The previous section showed that a square lattice does not offer a large TE band gap for the materials that Mr Bachmann could use to build up the photonic crystal samples. Therefore, the lattice structure is changed. Because the hexagonal lattice offers an even higher symmetry than the square one, the full TE band gaps were expected to be larger and more abundant.

The following results were computed for hexagonal lattices with size a and a single cylindrical rod in each unit cell. The rod is parallel to $\vec{a}_1 \times \vec{a}_2$, has a radius r and is made of a dielectric non-absorbing material with dielectric constant $\varepsilon = \varepsilon_r \varepsilon_0$. The unit cell is filled up with air.

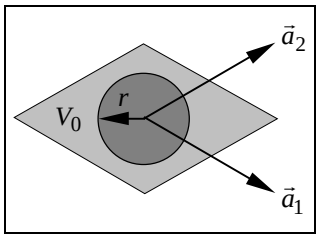

Image 12: Triangular lattice

Graph 6 shows the gap map. Note the greater number of band gaps and the more regular arrangement of the gap regions. In the 20th lowest bands, there is a full polarisation independent band gap region at $r \approx 0.35a$ and $f \approx 0.8c/a$. As expected, some larger TE band gap regions are present. An interesting TE region is found at $r \approx 0.16a$ and $f \approx c/a$.

Note that the bands are present at lower frequencies in the triangular lattice than the square lattice. This is due to the more compact hexagonal arrangement of rods – leading to an increased $\overline{\varepsilon_r}$ – hence, lower frequency.

Note also, that the nearly absence of large TE gaps is due to boundary conditions. Whereas the TM polarisation has its electric field $\vec{E}$ parallel to the *z*-axis and thus parallel to all material boundaries, the TE polarisation has $\vec{E}$ in the *xy*-plane, hence, in an arbitrary orientation to the material boundaries. From Maxwell's equations, it is deduced that the electric displacement $\vec{D}$ component perpendicular to a material boundary has to be continuous, whereas the parallel component is discontinuous in general. The results is that in a 2D photonic crystal, the frequency range for propagating TM modes is more constraint than the TE range.

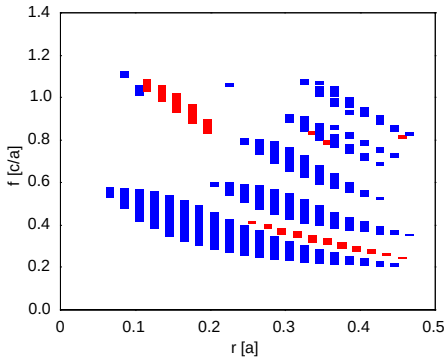

Graph 6: Gap map for $\varepsilon_r = 11$. TE band gaps in red and TM band gaps in blue.

4.3 Photonic crystal samples

Graph 6 showed the largest TE gap at $r = 0.18a$ for a hexagonal structure of cylindrical rods with $\varepsilon_r = 11$. This section details this particular configuration.

Band gap sample: wavelength filter

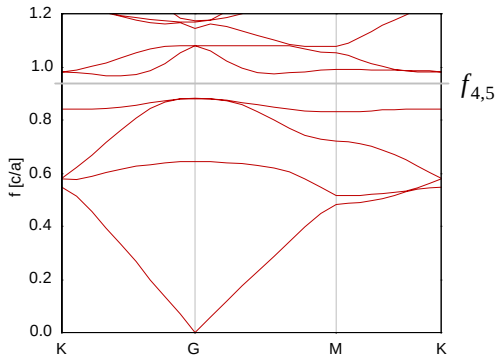

Graph 7: TE band structure for the 8th lowest photonic bands

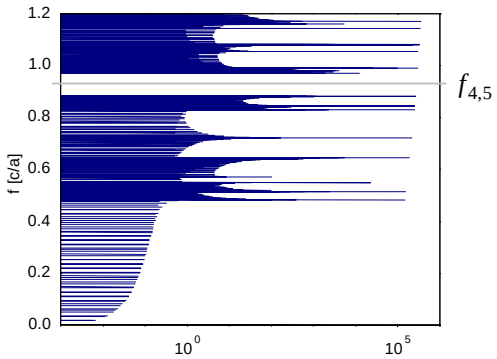

Graph 8: Approximate density of TE states (arbitrary scale in [s])

The crystal presents a gap from band 4 to band 5 with a mid-frequency $f_{4,5} = 0.92c/a$ and a relative extent

$g_{4,5} = 9.3\%$. Observe the high density of states for bands with a very low group velocity. These spikes could be particularly interesting for a low threshold laser, because of the strong electron–photon interaction (absorption, spontaneous and stimulated emission) due to the long presence of the photons.

For fabrication of the band gap sample, the HeNe laser wavelength needs to match $f_{4,5}$. Hence, the lattice constant is $a = 0.92\lambda_{HeNe} = 580\text{nm}$ and the cylindrical rods have a radius of $r = 0.18a = 105\text{nm}$.

Point defect sample: high Q cavity

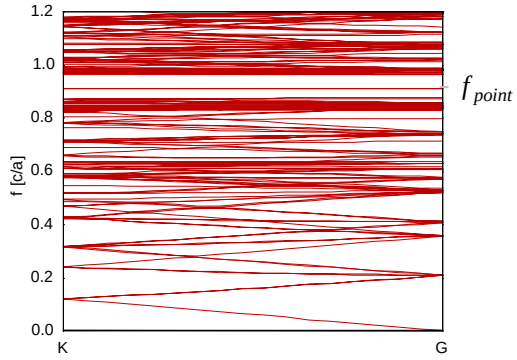

Graph 9: TE band structure for the 200th lowest photonic bands

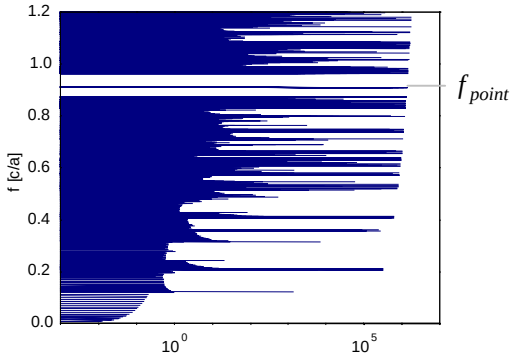

Graph 10: Approximate density of TE states (arbitrary scale in [s])

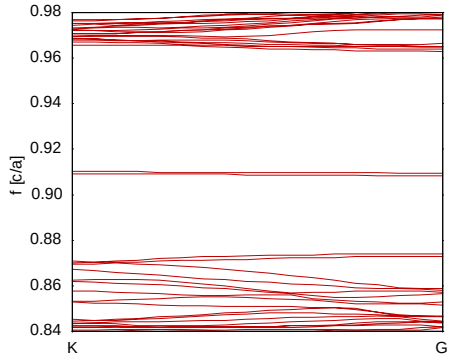

Graph 11: TE band structure around the two point defect bands

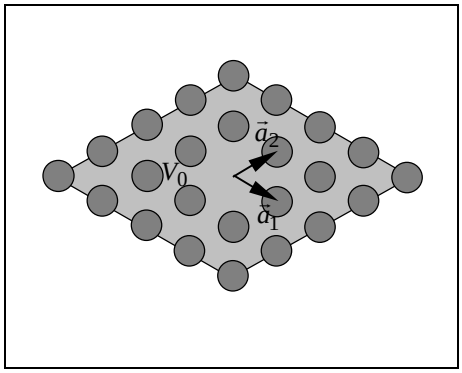

Image 13: Hexagonal 5x5 supercell with no central rod (point defect)

Image 13 shows the enlarged unit cell of the triangular lattice. The unit cell pattern is an exact copy of the band gap sample, but it lacks a single rod in the center. By the choice of a 5x5 supercell, the point defects are expected to be uncoupled, whereas the computational effort remains feasible [17]. Unfortunately, because of the 5x5 supercell, the 8 modes of the band gap sample are folded 25 times over and give rise to 200 modes in the same frequency range. It is possible to concentrate only on the defect modes and their neighbours to reduce computation time. Furthermore, if the defect modes are completely uncoupled, their group velocity is exactly zero – this means that the defect band is completely flat. Therefore, computation of just one *k*-point suffices in principle.

Graph 11 shows the frequency range around both defect modes at $f_{point} \approx 0.91c/a$. Indeed, the residual group velocity indicates a (very) weak coupling between the defect modes bound to neighbouring crystal defects. The energy of the defect mode remains mainly in the interior of its crystal defect. This is due to the heavy reflection of its wavelength, so that the photons cannot escape.

The defect modes can be considered as standing waves. For very low absorption, they create cavities with an extremely high quality factor – useful for telecom lasers or chronometers.

[17] The grid was set to a relatively small number *N*=128x128x1. But computation of 16 *k*-point took two days anyway.

Line defect sample: wave guide

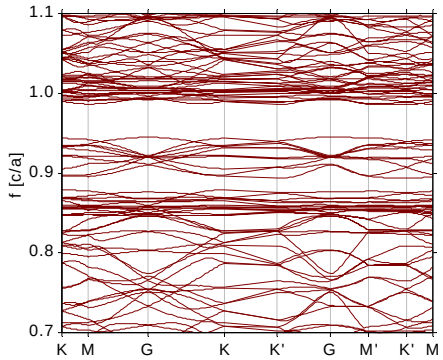

Graph 12: TE band structure around the line defect modes. The K' and M' points are *k*-points out of the line defect direction.

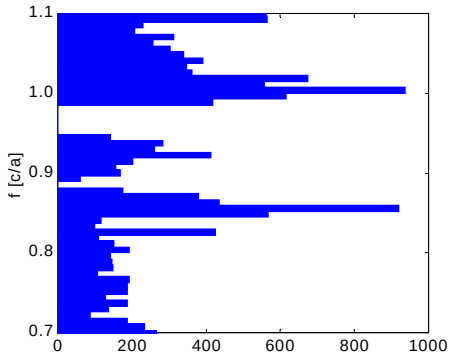

Graph 13: Approximate density of TE states (arbitrary scale in counts)

Image 14 shows the modified 5x5 supercell. Please note that the cylindrical rods have a relative dielectric constant $\varepsilon_r = 10$ rather than 11. This type of photonic crystal can be used as wave-guide for integrated optical devices, because it supports very small curvature radii to change the wave-guide direction [18].

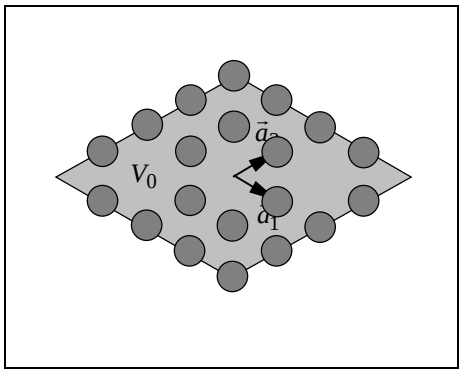

Image 14: Hexagonal 5x5 supercell with no central rods (line defect)

4.4 Absorption & limited size

If the dielectric material presents some absorption, this will reduce the strength of the retroaction due to the reduced mean lifetime of a photon. A similar effect can be expected for photonic crystals with limited size – for example a ten unit cells in each dimension instead of an infinity number.

The effect of weakened retroaction will be particular high for photonic crystals with already few retroaction (low ε-contrast). Then, it will smear out the photonic band frequencies, inducing a general decrease of band gap width. Smaller gaps may disappear completely.

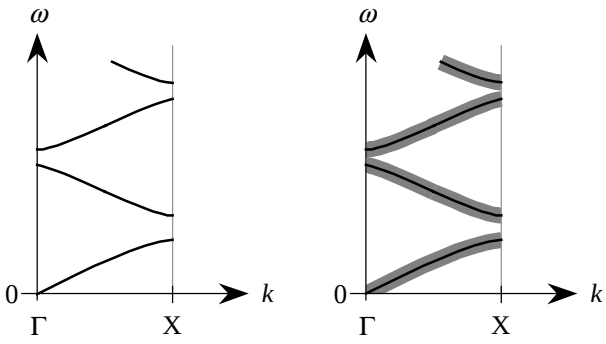

Graph 14: Band diagram for a 1D photonic crystal. At the left without and at the right with heavy absorption.

[18] See papers on "http://www.pbglink.com/".

5. Layout of photonic crystal samples

Mr Adrian Bachmann used an electron beam to deposit tips from an evaporated precursor. The deposition can be done on a conductive surface. Therefore, the glass substrate was previously covered by a thin ITO layer. The control system driving the electron beam presented a random lateral shift. This induced geometric aberrations and imposed an upper limit of deposition time. Hence, the photonic crystal had to be limited to less than a hundred tips.

The crystal is made of nearly cylindrical tips arranged regularly on the ITO surface. The tip head is of rather ellipsoidal shape, whereas its bottom is similar to an expanding cone. The tips were grown at about $2\lambda \ldots 3\lambda \approx 1.5\mu\text{m}$ height, so that the evanescent field is mainly located in their cylindrical range. Because of the surfacial location, the tips can be considered as cylindrical rods of infinite height for the evanescent wave. Hence, the photonic crystal is considered to be essentially bidimensional.

A HeNe laser beam internally reflected just below the photonic crystal creates the evanescent field. The wavelength is $\lambda = 633\text{nm}$.

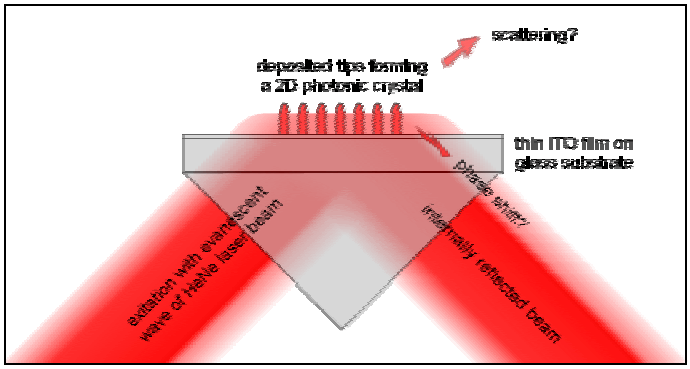

Image 15: Global design of the photonic crystal samples
It should be feasible to measure either the scattering (in transmission or reflection) or the phase shift induced by the total internal reflection (shearing interferometry with the help of the ITO layer).

5.1 Fabrication

Mr Bachmann used TEOS [19] as precursor, which has a complex refraction index $\tilde{n} = n + ik = 3.426 + i0.024$ at the HeNe laser wavelength. Fortunately, absorption is very low because the imaginary part is less than a percent of the real part of the refraction index. Hence, the computation for the sample crystals was made at $\varepsilon_r = 11 \approx |\tilde{n}|^2 = 11.8$ [20].

As mentioned above, because of random microscope shift during deposition, the number of rods per photonic crystal had to be limited. Image 16 shows a 9x5 hexagonal rod array with at maximum 41 tips. The crystal would cover a surface of about 3.6x6.0µm^2. By leaving out some marked tips, the layout can be easily modified to form the point and line defect sample instead of the simple band gap structure.

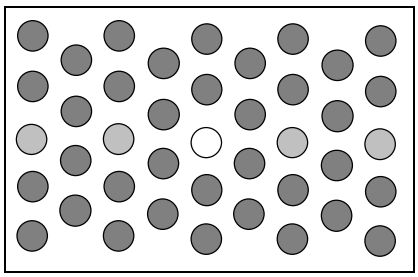

Image 16: Layout of the samples.
Point defect without the white rod, line defect without the light grey rods too.

6. Proposed measurement methods

It was previewed to evaluate the following methods experimentally. This part of the work was dropped because of the lack of a working photonic crystal sample. Nevertheless, some particular methods and the expected results are presented below.

19 Tetraethyl orthosilicate $C_8H_2O–O_4Si$ to form SiO_x by electron induced vapour deposition.
20 The measured value may have some undefined biased error – this means that the true value cannot exceed 11.8.

6.1 Transmission mode dark field microscopy

This idea has its reason in an earlier work [21], where a point defect in a photonic crystal had been imaged by reflection dark field microscopy.

It should be feasible to work in transmission mode. The effect of the photonic crystal defect may be a colour shift at the defect and an intensity change in scattered light.

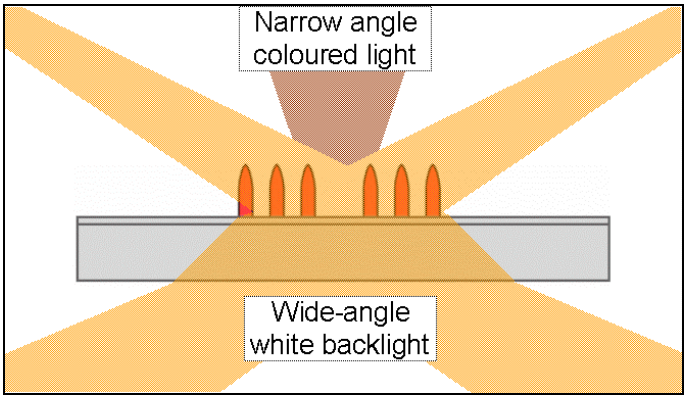

Image 17: Dark field microscopy to detect point defect.

6.2 Surface scattering of a HeNe laser backlight

Based on the experimental setup showed in image 15, the idea was to collect the scattered light over the photonic crystal and to determine the positions where particular high scattering occurs. If the laser beam creates an evanescent wave just on the left half of the crystal, scattering was expected to be mainly at the left if the wave falls in a band gap of the crystal. On the other hand, if the wave propagates in the crystal, scattering should manifest rather on the right half.

Either, the wave cannot really penetrate into the crystal (scattering at the left) or it propagates just to the right boundary and needs to leave the surface because the wave-guide stops (scattering at the right). Indeed, if the crystal accepts the wave, it may just not scatter at all – this would be the case if the presence of the crystal does not modify significantly the total internal reflection.

6.3 Back scattering and interference of a HeNe laser backlight

Image 18 shows the setup for a shearing interferometry measure. It is expected, that the acceptance of a mode by the photonic crystal expands its trajectory and enhances the Goos-Hänchen shift.

The experimental work should figure out if the idea is correct and to which extent the phase shift informs about the characteristics of the crystal's band structure.

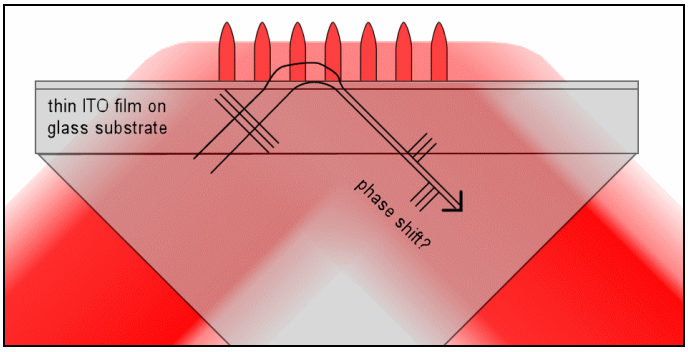

Image 18: Shearing interferometry by the ITO layer

[21] See annexe for a copy of the article "7x7 pattern with 600nm dot-to-dot distance Au-C pillars".

7. Summary

The functionality of the *MPB package* was tested and found quite powerful. The program was successfully installed on a personal workstation at home and on a server at school.

Some examples of photonic crystals were designed, but unfortunately, not yet produced and measured. So, the computational error was evaluated by convergence of the computation results. Indeed, with a planewave basis set of about 16 to 32 coefficients in each crystal dimension, the calculation error was estimated to remain below 5%.

In future, this work may be continued by:

- fabrication of the designed samples
- comparison of computed and measured behaviour
- try out of some other calculation software to quantitatively embed absorption, size limits, measurement methods and so on.

8. References

- K. Sakoda, "Optical Properties of Photonic Crystals": Springer-Verlag, Berlin/Heidelberg 2001
- Charles Kittel, "Einführung in die Festkörperphysik": 4th edition, R. Oldenburg Verlag, München/Wien 1976
- Steven G. Johnson, *The MIT Photonic-Bands Manual*: version 1.3, Massachusetts Institute of Technology, http://ab-initio.mit.edu/mpb/, visited on March 2002
- Steven G. Johnson and J. D. Joannopoulos, *Block-iterative frequency-domain methods for Maxwell's equations in a planewave basis*: Massachusetts Institute of Technology, http://ab-initio.mit.edu/, visited on March 2002
- Photonic band gaps, "http://www.pbglink.com/", visited on March 2002